Inelastic processes in ion-molecule collisions: Ar^+ and He^+ on N_2 at low-keV energies*

S. M. Fernandez,† F. J. Eriksen,‡ A. V. Bray,§ and E. Pollack
Department of Physics, University of Connecticut, Storrs, Connecticut 06268
(Received 31 March 1975)

The $Ar^+ + N_2$ collision is studied at energies from 1.0 to 3.0 keV and in an angular range between 0 and 4.0 deg. The energy-loss spectra of the scattered ions demonstrate the presence of elastic scattering and inelastic processes arising from vibro-rotational excitation of the ground electronic state of N_2, electronic excitation of the target with concomitant vibro-rotational excitation, and target ionization. Studies of the angular dependence of these processes suggest that (a) the collisions involve the entire molecule and are thus not adequately described in terms of a binary collision model, (b) electronic and vibrational excitation occur via mechanisms which exhibit negligible coupling, and (c) electronic excitation of N_2 is due predominantly to the $B\ ^3\Pi_g \rightarrow X\ ^1\Sigma_g^+$ transition as evidenced by observation of the onset of dissociation at larger scattering angles. The probability of charge exchange in $Ar^+ + N_2$ and $N^+ + N_2$ collisions is also investigated and shows an angular behavior very similar to that found in $He^+ + N_2$. Inelastic scattering results for $He^+ + N_2$ are reported.

I. INTRODUCTION

Experimental studies of the energy distributions of scattered ions as a function of scattering angle have in many cases provided information essential to our understanding of the dynamics of ion-atom collisions. The application of similar techniques to ion-molecule collisions (in the keV energy range) is more recent and, except for the work of Fayeton *et al.*,[1] who employed this approach to investigate scattering of N_2^+ by He, Ar, and Xe (0.3–3.0 keV), there is little work to cite in this respect. Studies of the energy distributions of ions scattered in the forward direction in ion-molecule collisions have been more numerous. By this method, Schowengerdt and Park[2] investigated the scattering of H^+, H_2^+, and Ar^+ by N_2 at relatively high energies (20–120 keV); Moore and Doering[3] studied H^+ and H_2^+ on N_2 at lower energies (150–500 eV), and Herrero and Doering[4] studied vibrational excitation of H_2 by protons (100–1500 eV).

Spectroscopic studies of collisionally induced optical radiation have been the most widely employed type for investigating inelastic ion-molecule collisions (particularly those employing N_2 as a target). Among the more relevant works are those of Polyakova *et al.*[5-7] and Moore and Doering,[8-10] dealing with vibrational and rotational excitation of N_2 by several atomic and molecular ions ranging in energy from 0.4 to 37 keV. Moore and Doering have found that for projectile-ion velocities greater than 10^8 cm sec^{-1}, the relative band intensities of the $\Delta v = -1$ sequence of the first negative system in N_2^+ ($B\ ^2\Sigma_u^+ \rightarrow X\ ^2\Sigma_g^+$) agree with the predictions of the Franck-Condon principle, while Polyakova and co-workers report excitation of the $B\ ^2\Sigma_u^+$ state of N_2^+ with violation of the Franck-Condon principle (3–37 keV).

In this paper we report[11] results of our studies on the $Ar^+ + N_2$ and $He^+ + N_2$ systems, performed by energy-analyzing the scattered ions at select scattering angles and at several incident-beam energies (1.0–3.0 keV). In addition, measurements of the probability of electron capture as a function of scattering angle for both Ar^+ and N^+ on N_2 are made to determine the relative importance of the direct versus charge-exchange scattering. Similar results on electron capture in $He^+ + N_2$ collisions have already been published.[12]

A detailed understanding of ion-molecule interactions is of interest from both theoretical and practical standpoints, and should prove valuable in explaining many physical phenomena at a fundamental level. Theoretical interest arises because many of the approximations commonly employed in the treatment of these collisions are valid at either lower energies (less than 50 eV) or at higher energies (above 20 keV), but are not satisfactory at intermediate values. An understanding of these interactions is also of interest in relation to auroral and afterglow phenomena.[13-15]

II. EXPERIMENTAL METHOD

The basic apparatus has been previously described in detail[16,17] and is shown schematically in Fig. 1. The ions which are produced by electron bombardment in the ion source are extracted, momentum-selected (with an attendant change in direction of 90°), accelerated by a series of potential gradients, and focused into a beam by an ion-optics system employing cylindrical electrostatic lenses. Energy analysis of the scattered ions is performed electrostatically with a 5-in. parallel-plate ana-

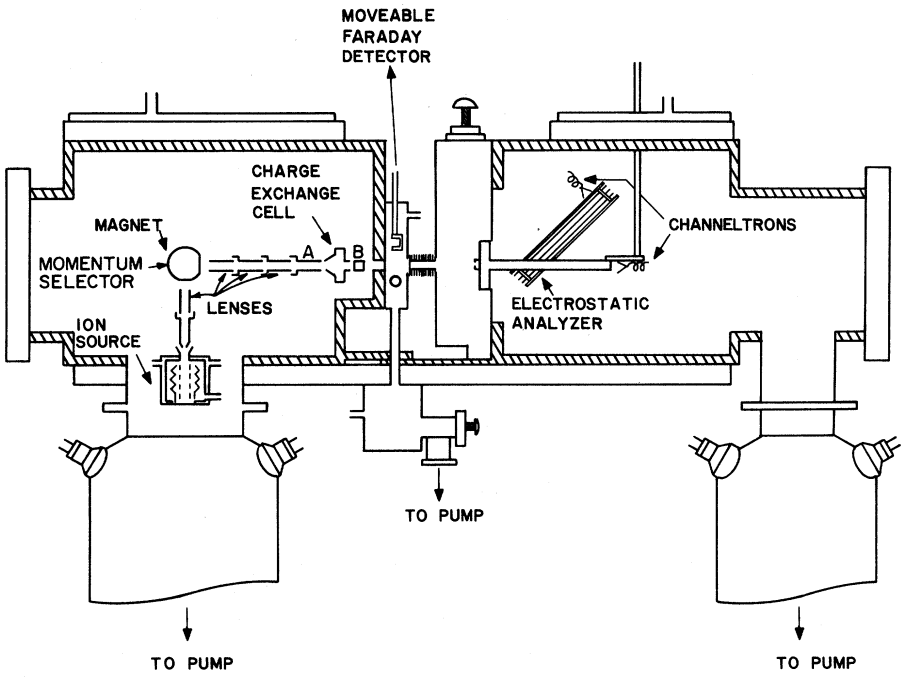

FIG. 1. Schematic of the apparatus.

lyzer. An exit aperture on its back plate allows undeflected neutral particles to pass through. During operation, the front plate is maintained at ground potential while the voltage on the back plate is varied. Channeltron electron multipliers located at each exit slit of the analyzer detect the energy-analyzed ion signal and the undeflected neutral component of the scattered signal.

For studies of direct scattering, the entrance and exit slits of the analyzer are set at widths of 0.0016 and 0.0010 in., respectively. These settings result in a theoretical energy resolution of 5×10^{-4}. Figure 2 shows typical energy profiles of the incident beam (no scattering gas) taken at two different angular resolutions at an incident beam energy of 2.0 keV. For measurements of probability of electron capture, both slits are kept fully opened (0.25 in.).

The experiments are performed by scattering a well-defined beam of quasi-monoenergetic ions by N_2 (research grade) target molecules. Measurements are made under single-collision conditions. The scattered ions are energy-analyzed, and energy-loss spectra (ELS) are obtained by a multiscaling technique which has been described in detail elsewhere.[18] This technique employs a digital logic circuit which steps the analyzer voltage by a discrete amount and simultaneously advances the channel of a multichannel analyzer each time a preset number of neutral particles is detected. Upon completion of one full sweep (128 channels), the scanner resets back to the starting scan voltage

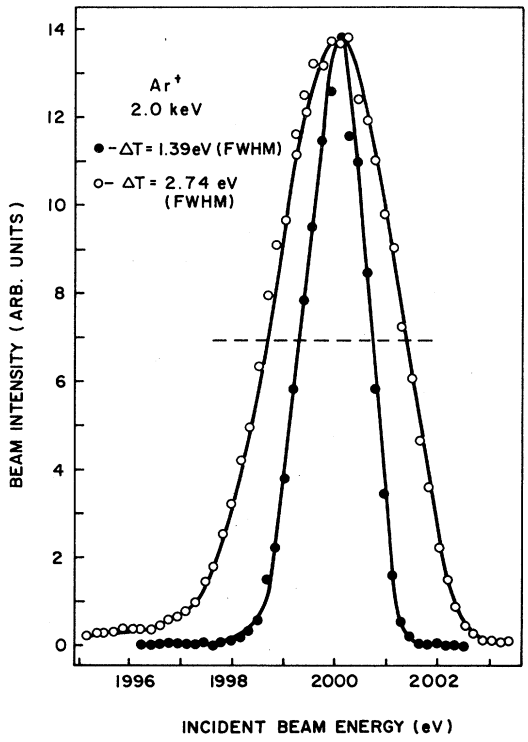

FIG. 2. Incident-beam energy profiles taken at two different angular resolutions. High (●) and low (○) angular resolutions were employed to obtain the small- ($0<\theta<1.0$) and large- ($1.0<\theta<4.0$) angle data, respectively. The beam collimation systems employed yield incident-beam half-widths of 0.1 and 0.25 degrees.

and a new accumulation cycle takes place, or accumulation stops and the information stored in the multichannel scaler is printed by teletype and/or plotted by an X-Y recorder. The energy analyzer was calibrated by observing known transitions in $Ar^+ + Ar$ collisions.[17]

The results obtained by the procedure outlined above are in the form of ELS at selected scattering angles and at several impact energies. These spectra represent scattered-ion intensity vs ΔE, the energy loss. The inelastic energy loss Q, which is the quantity of physical interest in these experiments, is not directly obtainable from the spectra, and its determination requires additional kinematic considerations. In the ion-atom case the procedure is straightforward, and the conservation of energy and momentum equations allow a unique determination of Q. In the ion-molecule case the matter is not so simple, since the necessary conservation equations depend on the target mass, and inelastic scattering from a molecule is viewed, in different theoretical models, as occurring either with the entire molecule or with one of its atoms. This problem is discussed below, and the collision is shown to occur with the entire molecule.

III. RESULTS AND DISCUSSION

A. Charge transfer

The angular dependence of P_0, the probability of charge transfer (defined as the ratio of the scattered neutral to scattered total signal at a fixed scattering angle) is investigated for the $Ar^+ + N_2$ collision. The technique used in these measurements was previously described,[12] and P_0 is found to exhibit the same qualitative behavior as in $He^+ + N_2$.[12] P_0 increases monotonically with increasing scattering angle and then maintains a relatively constant value with further increase in angle, as may be seen in Fig. 3(a). The purpose of the P_0 measurement is to ascertain the relative importance of direct vs charge-exchange scattering. It is noteworthy that in most of the angular region studied, charge-transfer processes in $Ar^+ + N_2$ occur in approximately one-half the collisions. Charge exchange in $N^+ + N_2$ is also studied and, as shown in Fig. 3(b), the same behavior is found in P_0.

B. Collision model

Consider a collision between a projectile C and a homonuclear diatomic molecular target AB. In general, the total momentum $\vec{P}$ transferred to AB is

$$\vec{P} = \vec{P}_A + \vec{P}_B , \tag{1}$$

where $\vec{P}_A$ and $\vec{P}_B$ are the momenta transferred to each atom. The amount of projectile kinetic energy converted into internal energy of excitation of the molecule (Q) is equal to the sum of the kinetic energies of A and B in a frame fixed on the center of mass of AB, and therefore

$$Q = [2(P_A^2 + P_B^2) - P^2]/4M, \tag{2}$$

where M in the present case is the mass of the nitrogen atom.

Two interesting limiting cases arise. One is that of a "binary" encounter between A and C, in which B is a simple spectator.[19-22] The momentum transfers here are $\vec{P}_A = \vec{P}$ and $\vec{P}_B = 0$, and therefore $Q = P^2/4M$. Momentum transfer during the collision occurs only between the projectile and one of the atoms of the target molecule. The transfer of kinetic energy from the projectile to internal degrees of freedom of the molecule (assuming no electronic excitation for the moment) can then be construed as taking place in two steps. The first step consists of a binary elastic collision between the projectile and one of the atoms of the molecular target, with scattering and recoil at angles con-

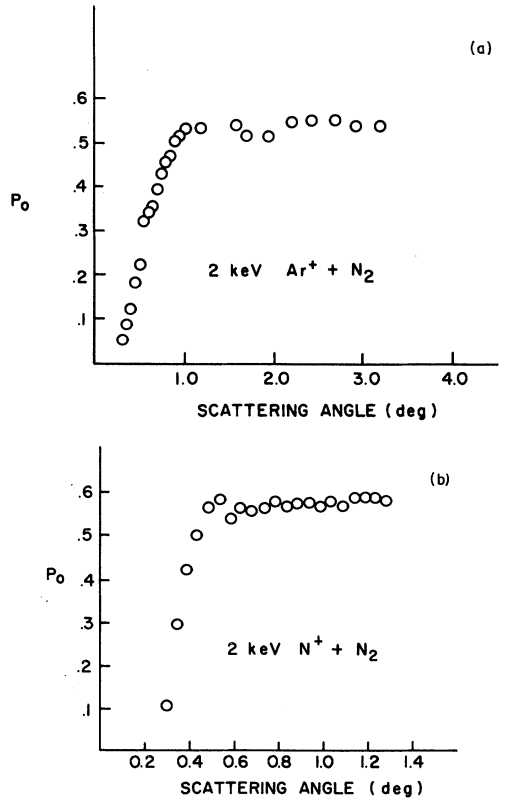

FIG. 3. Probability of charge exchange as a function of of scattering angle (a) 2.0 keV—$Ar^+ + N_2$; (b) 2.0 keV—$N^+ + N_2$.

sistent with conservation of momentum and energy for this elastic collision. The second step involves the partition of the kinetic energy transferred to the one atom of the molecule into internal vibro-rotational excitation of the molecule and translational kinetic energy of its center of mass.

The other limiting case arises when it is assumed that the two atoms A and B of the target molecule are rigidly bound. In this case, the collision can only be purely elastic (neglecting electronic excitation). For brevity, this case will be referred to in what follows as the "limiting elastic" case.

It is well known that certain general features of experimental results on vibrational dissociation of diatomic molecules by ion and atom impact at energies higher than those of the present study[23,24] can be explained, at least qualitatively, in terms of the binary-encounter limiting case, sometimes referred to as "spectator stripping mechanism" collisions. It is thus of interest to compare our results with the predictions of the two limiting cases discussed above. These predictions take a particularly simple form in the collision system studied, for the particle detected in this case is the scattered ion, which obviates the need to take explicit account of the partitioning of energy in the recoiling molecule.

In the binary limiting case the energy loss ΔE of the scattered projectile (of mass M_p), for small scattering angles θ, can be approximated by the expression[25]

$$\Delta E_{\text{bin}} \approx (M_p/M)E_0\theta^2 , \tag{3}$$

where E_0 is the energy of the incident ion and M is the mass of the nitrogen atom. In the limiting elastic case, on the other hand,

$$\Delta E_{\text{el}} \approx (M_p/2M)E_0\theta^2 . \tag{4}$$

Equations 3 and 4, when plotted as ΔE vs $E_0\theta^2$, yield straight lines of slopes M_p/M and $M_p/2M$. Energy-loss spectra of Ar^+ ions scattered by N_2 exhibit two peaks and a shoulder (labeled A, B, and C, respectively) whose positions shift towards higher energy losses as θ increases. The interpretation of these peaks will be presented in detail below. For the moment, let it suffice to state that peak A is associated both with elastic scattering and vibro-rotational excitation of the ground electronic state of the target; peak B reflects electronic excitation of the target with concomitant vibro-rotational excitation, and peak C is identified as arising from ionization of the target. A plot of the most probable value of ΔE vs $E_0\theta^2$ for each of these peaks is shown in Fig. 4 for beam energies of 1.0, 2.0, and 3.0 keV. This figure also shows plots of Eqs. (3) and (4) labeled "binary limit" and "elastic limit," respectively. It is evident from Fig. 4 that our results for peak A lie on a straight line of slope intermediate between those predicted by the two limiting cases, and thus are not consistent with the assumption of a binary encounter, which would require the data points to lie on the upper curve. Instead, these results can be explained in terms of inelastic collisions involving the entire molecule. The difference between the actual data points at any given value of $E_0\theta^2$ and the curve labeled "elastic limit" is then equal to Q, the internal energy of excitation of the molecule.

It is interesting to note at this point that the curves for peaks B and C plotted in Fig. 4 follow straight lines with the same slope as that of peak A. This suggests that the mechanism of vibro-rotational excitation is the same in those processes which involve electronic rearrangement in the molecule. This phenomenon will be discussed further below.

The fact that our results are not well described in the binary limit is not surprising. In general, it would be expected that binary encounters occur

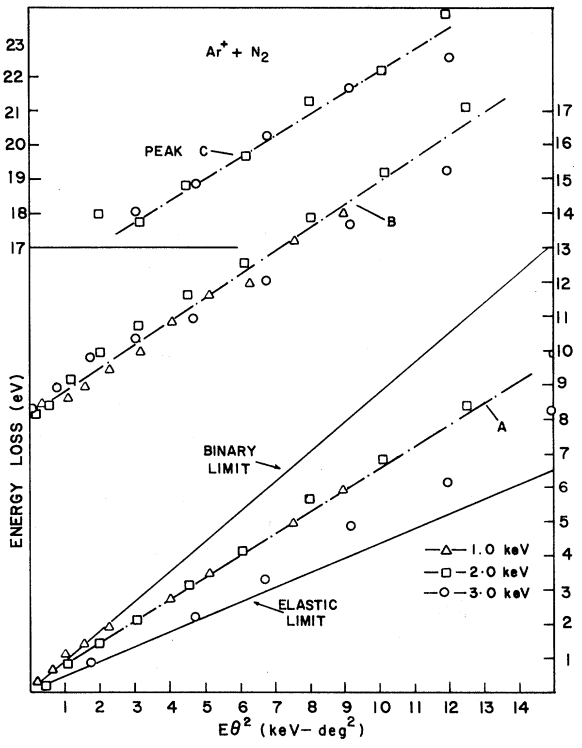

FIG. 4. Most probable energy losses of Ar^+ for peaks, A, B, and C, vs $E_0\theta^2$, where E_0 is the incident projectile energy and θ is the laboratory scattering angle. See Fig. 5 and the text for explanation of the various peaks. The predictions of binary and elastic models for the collision (see text) are also included for comparison.

in the limiting case of a vanishing molecular bond between the atoms of the molecule. This condition may be fulfilled at higher impact energies when the energy transferred to the target particle greatly exceeds the bonding energy. A simple calculation shows that in the typical case of 0.01-rad ($\theta \approx 0.6°$) scattering of a 2.0-keV Ar^+ ion by a stationary N_2 target (assuming a binary encounter), the kinetic energy acquired by a nitrogen atom is of the order of 0.5 eV. This energy is of the same order of magnitude as the spacing of vibrational levels of N_2 and shows why the binary limit does not provide an adequate description of the collision process.

C. $Ar^+ + N_2$

The energy-loss spectra for $Ar^+ + N_2$ are characterized by two peaks and a shoulder (labeled A, B, and C in Fig. 5) whose relative magnitudes change substantially in the angular range studied, indicating the onset and increased role of inelastic channels as θ increases. For example, at 2.0 keV, $\theta = 0.5°$, the intensity at the maximum of peak A is about 200 times larger than that of peak B, whereas at $\theta = 1.25°$ they are approximately equal and at $\theta = 3.0°$ the magnitude of peak B is about twice that of A. Quantitative comparison of the heights of peaks B and C relative to that of peak A at scattering angles smaller than 0.5° is not justified, since the data may contain contributions from the unscattered incident beam at these small angles. The widths of the various peaks are also found to increase as the scattering angle gets larger.

a. Peak A. At the smallest angles of scattering studied, peak A corresponds to elastically scattered ions ($Q = 0$). Q is found to increase monotonically with increasing θ as shown in Fig. 6, and at $\theta = 3.5°$ it attains a value of 4.5 eV. The gradual shift of peak A with scattering angle and the fact that the lowest excited electronic state of N_2 ($A\,^3\Sigma_u^+, v = 0$) is 6.3 eV above the ground state, permit the unambiguous identification of peak A with vibro-rotational excitation of the molecule in its ground electronic state and indicates that energy transfer becomes more effective as the angle of scattering increases. Although in our present study vibrational excitation cannot be distinguished from rotational excitation, the term "vibro-rotational excitation" is employed because indirect evidence suggests that considerable rotational excitation may be taking place. Moore and Doering[8-10] have observed non-Boltzmann rotational distributions in the first negative system of N_2^+ when excited by ion impact at incident velocities less than 10^8 cm sec^{-1}. Their results, however, must be extrapolated to our case with caution, since by the nature of their experimental technique they were restricted to observing ionizing and/or charge-transfer collisions in an energy range where the cross section for charge transfer is about an order of magnitude larger than the ionization cross section.[26] In a more recent study already mentioned, Herrero and Doering failed to detect any rotational excitation of H_2 by proton impact.

b. Peak B. Peak B is interpreted as arising from electronic excitation of the target N_2, as there are no states of Ar^+ that could account for this feature. In addition, peak B is also observed in the case of He^+ impact. The discrete nature and distinct separation of peak B from peak A indicate that electronic excitation is a rather specific process.

The identification of electronic transitions in terms of known states of N_2, however, is obscured by the fact that N_2 has many overlapping states in the range of energies corresponding to the positions of peak B; thus, only tentative assignments can be made.

The identification of the participating states may be guided by the Franck-Condon principle. It is well known that in the case of electron-molecule collisions at impact energies greater than 100 eV, good agreement is found between experimental results and the predictions of the Franck-Condon principle.[27,28] Although studies of ion-molecule collisions at various energies have yielded results that are not always consistent, we find it worthwhile to discuss our results within this context.

At 2.0 keV and for forward scattering, our data show a small inelastic peak with a maximum intensity at 8.1 eV. Two states of N_2, the $A\,^3\Sigma_u^+$ and the $B\,^3\Pi_g$, are the most likely to account for this feature (see Fig. 7). Franck-Condon factors predict maxima at 7.7 eV for the $A \rightarrow X$ transition and 7.9 eV for the $B \rightarrow X$ transition.[29,30] Several considerations discussed below argue in favor of the dominance of the B state.

As with peak A, the value of Q at the maximum-intensity position of peak B increases monotonically with scattering angle. This shift of peak B toward higher energy losses can be interpreted in two ways. It can be viewed as reflecting transitions to higher electronic states, so that at larger scattering angles peak B represents the unresolved contributions of several electronic states, or alternately, as excitation to the same electronic state with increased vibrational and rotational excitation, or a combination thereof.

In an attempt to resolve this question, selected ELS were curve-fitted by sums of Gaussian distributions (maximum of five) properly skewed to match the energy distribution of the incident ions.

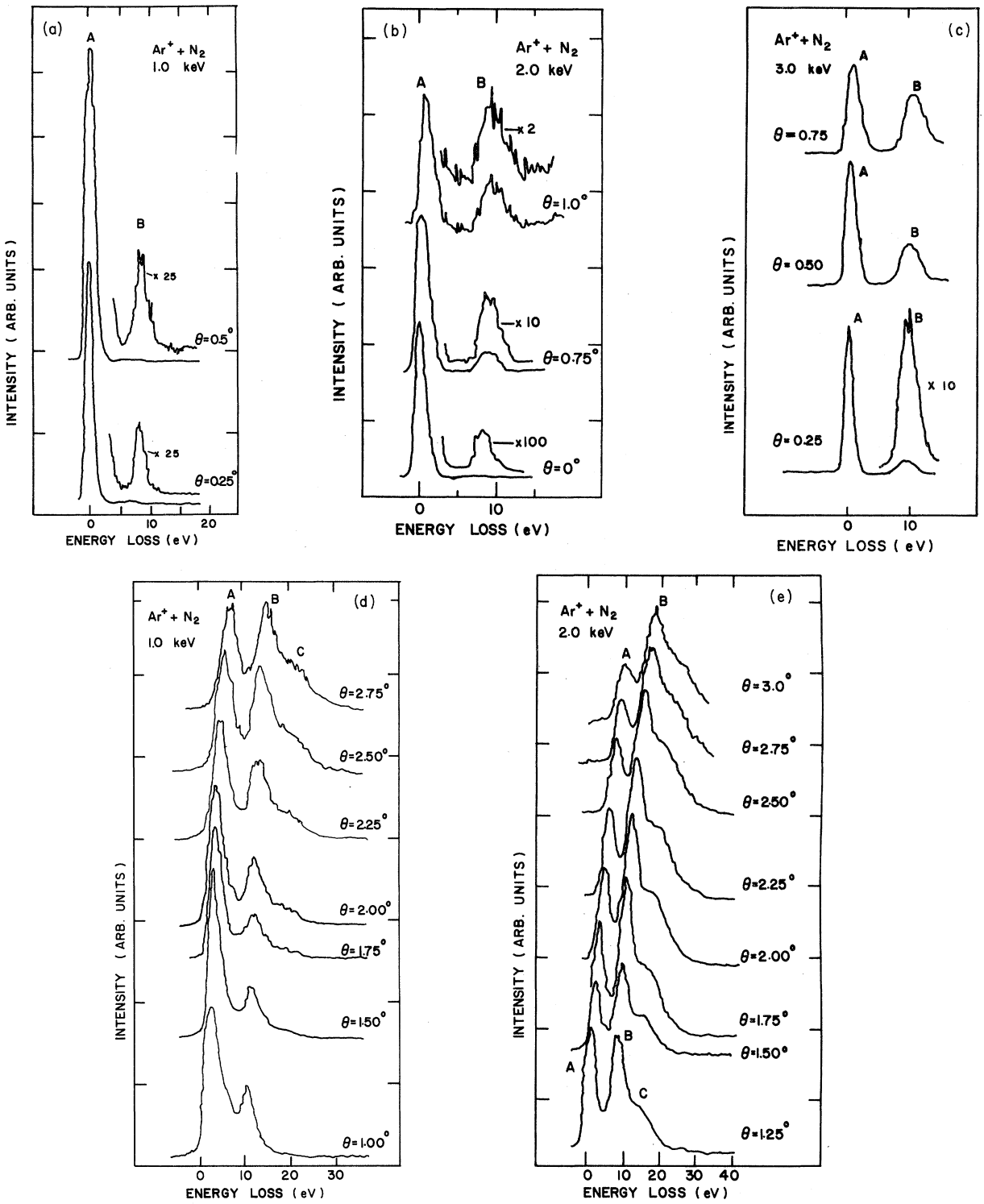

FIG. 5. Energy-loss spectra for $Ar^+ + N_2$ collisions. Small-angle, high-resolution data are shown in (a), (b), and (c). Large-angle data are shown in (d) and (e). While only two peaks (A and B) are seen in the small-angle data at all energies studied, the large-angle data reveal an additional shoulder, labeled C. A shift in the positions of these peaks towards higher energy losses as θ increases is readily seen from these plots. It is also apparent that the collisions, which are predominantly elastic at low energy and small angles, become predominantly inelastic at higher energies and angles.

In all cases tried, a best fit is obtained with three Gaussians, provided the one corresponding to peak C was skewed further toward higher energy losses.

The results of this analysis suggest then that peak B arises predominantly from excitation to a single electronic state. Additional, and perhaps more significant, substantiating evidence for this hypothesis can be obtained from Figs. 4 and 6, which show ΔE versus $E_0\theta^2$ and Q versus θ, respectively, for peaks A, B, and C. It can be seen from these figures that the separation between curves A and B is constant at about 8 eV. Since curve A represents pure vibro-rotational excitation, the constant separation of curve B strongly argues in favor of the idea that the shift in peak B with scattering angle is due to increased vibro-rotational excitation accompanying the same electronic transition, and not to excitation of higher electronic states.

If the above interpretation is correct, the shape of peak B should change noticeably at the onset of dissociation, i.e., when vibrational dissociation of the electronic state in question begins to occur, peak B should change from a well-defined peak to one with a sharp onset but with a slowly tapering tail. Since the dissociation limit of the A state is 9.7 eV and that of the B state is 12.1 eV,[29] this feature provides a means to distinguish between states A and B. Careful inspection of the ELS in Fig. 5 shows that the onset of dissociation is in fact observed, and that it is not until Q is about 12.5 eV that a noticeable change appears ($\theta = 2.75°$ at 2.0 keV). At $\theta = 3.0°$, Q is 13 eV, and the falloff of this peak is so gradual that peak C is no longer distinguishable as a separate feature. On the basis of this evidence it appears that the B state provides the main contribution to peak B, although some excitation to other close-lying states cannot be completely ruled out.

Our results then indicate that, at least for the forward direction, electronic excitation occurs according to the predictions of the Franck-Condon principle. The excess vibrational energy observed at larger scattering angles may be taken to indicate breakdown of the Franck-Condon principle, since the nuclei apparently do gain appreciable momentum during collisions resulting in electronic transitions. This view, however, needs further elaboration, since the constant separation of peaks A and B suggests that vibrational excitation in these collisions occurs via a mechanism which is independent of the electronic excitation process.

A collision model which is consistent with our results views the interaction manifested by peak B as taking place in two independent steps: (a) an electronic transition to the B state in agreement with the predictions of the Franck-Condon principle, and (b) vibrational excitation of the electronically excited molecule. The increased width of peak B relative to that of peak A at a given angle may be attributable to differences in the shape of the potential energy curves of the ground and B electronic states.

Russek[31] has recently treated this problem theoretically, and has found that a second-order Born-approximation treatment of the collision in fact predicts negligible coupling between the vibrational

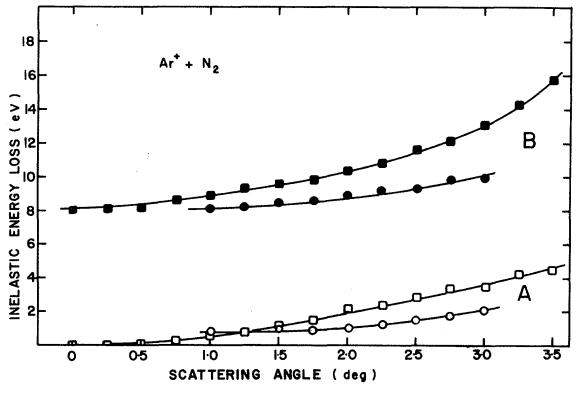

FIG. 6. Inelastic energy loss Q vs scattering angle for $Ar^+ + N_2$ at 1.0 keV (circles) and 2.0 keV (squares) as calculated from the positions of the peaks A and B in the energy-loss spectra.

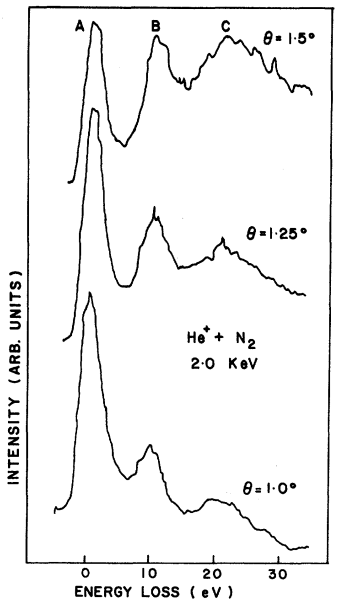

FIG. 7. Energy-loss spectra for $He^+ + N_2$ collisions at 2.0 keV. As in the case of $Ar^+ + N_2$, three peaks can be seen whose positions and relative heights change dramatically with scattering angle.

and electronic excitation mechanisms.

c. Peak C. The feature labeled *C*, which appears as a shoulder in the ELS, is attributed to ionization of the target N_2. This feature is not observed in the small-angle data. At 2.0 keV, $\theta = 1.25°$, its position corresponds to a Q value of 16.2 eV, and as the scattering angle increases it shifts monotonically towards higher energy losses, as seen in Fig. 5. The results of fitting a typical ELS with a sum of Gaussian distributions shows that the Gaussian required to fit peak *C* is skewed toward higher energy losses. This is what would be expected for an ionization process, in which the detached electron may carry off kinetic energy.

The observed Q of 16.2 eV at the smallest angle at which peak *C* appears in our results implies that the ionized target is left in its ground state $X^2\Sigma_g^+$. In a ΔE vs $E_0\theta^2$ plot (Fig. 4), the curve corresponding to peak *C* has the same slope as those corresponding to peaks *A* and *B*. As discussed earlier, this suggest that the shift in position of peak *C* with scattering angle is due to increased vibrational excitation of the same electronic state with increasing scattering angle.

D. $He^+ + N_2$

Energy-loss spectra are obtained from $He^+ + N_2$ collisions at 1.0, 2.0 and 3.0 keV, and are found to resemble those of $Ar^+ + N_2$ in their salient features. Figure 7 shows typical spectra at a beam energy of 2.0 keV and several scattering angles. Because the data for He^+ are not as extensive as for Ar^+, an analysis as detailed as that presented for the latter system is not possible in this case. Nevertheless, it seems clear that the same basic interpretation applies to peaks *A*, *B*, and *C*, i.e., vibro-rotational excitation, electronic excitation, and ionization of the target, respectively.

Although they are basically similar, comparison of the ELS from $Ar^+ + N_2$ and $He^+ + N_2$ collisions reveals some differences. For example, at a given energy, the Q's observed at each scattering angle are slightly larger in the case of He^+ impact. On the basis of the available data, it is not possible to ascertain whether this is due to excitation to higher electronic states or simple due to increased vibrational excitation accompanying the same electronic transitions as seen in the case of Ar^+ impact. A more marked difference between the ELS of He^+ and Ar^+ becomes evident upon comparison of the relative heights of the various peaks. For instance, for He^+ at 2.0 keV, $\theta = 1.5°$, peaks *A*, *B*, and *C* have approximately the same height, with peak *C* contributing the largest area. In the case of Ar^+ impact at the same energy and angle, peak *A* has the smallest relative height.

Finally, in the case of He^+ impact, peak *C* appears as a well-defined broadened peak rather than a shoulder, as was found to be the case for Ar^+ impact. This peak is attributed to ionization of the target, since no state of He^+ can account for the energy losses observed for peak *C*.

---

*Supported by the U. S. Army Research Office-Durham, the University of Connecticut Research Foundation, and the Connecticut Research Commission.

†Present address: Health Center, University of Connecticut, Farmington, Conn. 06032.

‡Present address: Behlen Laboratory of Physics, University of Nebraska, Lincoln, Neb. 68508.

§Present address: Planning Systems Inc., McLean, Va. 22101.

[1] J. Fayeton, A. Pernot, P. Fournier, and M. Barat, J. Phys. (Paris) 32, 743 (1971).

[2] F. D. Schowengerdt and J. T. Park, Phys. Rev. A 1, 848 (1970).

[3] J. H. Moore, Jr. and J. P. Doering, J. Chem. Phys. 52, 1692 (1970).

[4] F. A. Herrero and J. P. Doering, Phys. Rev. A 5, 702 (1972).

[5] V. A. Gusev, G. N. Polyakova, and Ya. M. Fogel', Zh. Eksp. Teor. Fiz. 55, 2128 (1968) [Sov. Phys.—JETP 28, 1126 (1969)].

[6] G. N. Polyakova, Ya. M. Fogel', J. F. Erko, A. V. Zats, and A. G. Tolstolutskii, Zh. Eksp. Teor. Phys. 54, 374 (1968) [Sov. Phys.—JETP 27, 201 (1968)].

[7] G. N. Polyakova, Ya. M. Fogel', and A. V. Zats, Zh. Eksp Teor. Fiz. 52, 1495 (1967) [Sov. Phys.—JETP 25, 993 (1967)].

[8] J. H. Moore, Jr. and J. P. Doering, Phys. Rev. 174, 178 (1968).

[9] J. H. Moore, Jr. and J. P. Doering, Phys. Rev. 182, 176 (1969).

[10] J. H. Moore, Jr. and J. P. Doering, Phys. Rev. 177, 218 (1969).

[11] S. M. Fernandez, F. J. Eriksen, A. V. Bray, and E. Pollack, in *Eighth International Conference on the Physics of Electronic and Atomic Collisions, Abstract of Papers, Belgrade, 1973* (Institute of Physics, Belgrade, 1973), p. 168.

[12] S. M. Fernandez, F. J. Eriksen, and E. Pollack, Phys. Rev. Lett. 27, 230 (1971).

[13] K. C. Clark and E. Beton, J. Atmos. Terr. Phys. 16, 205 (1959).

[14] D. Barbier and D. R. Williams, J. Geophys. Res. 55, 401 (1950).

[15] A. Ombolt, *The Optical Aurora* (Springer-Verlag, New York, 1971).

[16] S. W. Nagy, S. M. Fernandez, and E. Pollack, Phys. Rev. A 3, 280 (1971).

[17] F. J. Eriksen, S. M. Fernandez, A. V. Bray, and E. Pollack, Phys. Rev. A 11, 1239 (1975).

[18] A. V. Bray, F. J. Eriksen, S. M. Fernandez, and E. Pollack, Rev. Sci. Instrum. 45, 429 (1974).

[19] V. I. Gerasimenko and Yu. D. Oksyuk, Zh. Eksp. Teor.

Fiz. 48, 499 (1965) [Sov. Phys.—JETP 21, 333 (1965)].
[20]T. A. Green, Phys. Rev. A 1, 1416 (1970).
[21]H. Van Dop, A. J. H. Boerboom, and J. Los, Physica 61, 616 (1972).
[22]J. Baudon, J. Phys. B 6, 850 (1973).
[23]D. K. Gibson, J. Los, and J. Schopman, Physica 40, 385 (1968).
[24]H. Van Dop, A. J. H. Boerboom, and J. Los, Physica 54, 223 (1971).
[25]S. M. Fernandez, Ph.D. thesis (University of Connecticut, 1975) (unpublished).
[26]W. F. Sheridan, O. Oldenberg, and N. P. Carleton, in Second International Conference on the Physics of Electronic and Atomic Collisions, Abstracts of Papers, Boulder, Colorado, 1961, p. 159.
[27]E. N. Lassettre and M. E. Krasnow, J. Chem. Phys. 40, 1248 (1964).
[28]E. N. Lassettre, A. Skerbele, and V. D. Meyer, J. Chem. Phys. 45, 3214 (1966).
[29]F. Gilmore, J. Quant. Spectrosc. Radiat. Transfer 5, 369 (1965).
[30]W. Benesch, J. T. Vanderslice, S. G. Tilford, and P. G. Wilkinson, Astrophys. J. 142, 1227 (1965).
[31]A. Russek (personal communication).